Ionospheric-Constrained PPP using Triple-GNSS Constellations

Robert S.B. Galatiya SUYA, Malawi

Key words: Triple-GNSS, PPP, Ionosphere-constrained, Standard PPP

SUMMARY

The technique of Precise Point Positioning (PPP) has wide-spread application in positioning, navigation, and timing (PNT) due to its improved accuracy and low cost. However, the technique continues to suffer from long convergence period in order to attain Real-Time Kinematic (RTK) comparable performance. The fusion of multi-GNSS constellations remains today's most probable remedy to the long convergence time with improved positioning accuracy, availability, redundancy and integrity. Besides, the Ionosphere and Hardware Delay (IHD) derived from Global Ionosphere Maps (GIM) generated by the International GNSS service (IGS) have proved significant in accelerating single-frequency PPP convergence time. Previous literature has a deficiency on triple constellation PPP incorporating both ionosphere-constrained single frequency PPP and dual-frequency PPP. In this paper, GPS+GLONASS+Galileo GNSS constellations are evaluated in kinematic mode over nine (9) Multi-GNSS Experiment (MGEX) stations. Twenty-four (24) hour observations for the first week of February, 2017 are processed in four PPP scenarios (GPS-only, GLONASS-only, GPS+GLONASS, and triple-constellation of GPS+GLONASS+Galileo) at 7° elevation angle cut-off. To validate the findings, standard single-frequency PPP and dual-frequency PPP are analyzed. The results indicate that the application of GIM in ionosphere-constrained PPP improves the overall convergence time and standard deviation with respect to standard single-frequency PPP. Furthermore, better convergence time is obtained in dual-frequency PPP without virtual observations. Moreover, augmenting GPS with GLONASS and Galileo, triple-constellation, improves in relation with GPS-only PPP in standard single-frequency PPP, standard dual-frequency PPP, and in ionosphere-constrained PPP. Thus, this study fills the gap in literature by unveiling the threshold of performance for the ionosphere-constrained PPP using triple-GNSS constellations.

Ionospheric-Constrained PPP using Triple-GNSS Constellations (9769)
Robert Suya (Malawi)

FIG Working Week 2019
Geospatial information for a smarter life and environmental resilience
Hanoi, Vietnam, April 22–26, 2019

Ionospheric-Constrained PPP using Triple-GNSS Constellations

Robert Galatiya S.B. SUYA, Malawi

1. INTRODUCTION

Precise Point Positioning (PPP) is a versatile tool which provides sub-centimetre and decimetre-level accuracy in in static and kinematic modes, respectively (Huber et al., 2010; Vollath et al., 2000; Zumberge et al., 1997). PPP plays a greater in geo-physical geodesy, remote sensing of the ionosphere (Ren et al., 2016) and atmosphere (Li, et al., 2015), space and fundamental physics and engineering disciplines of surveying, navigation, and timing.

Performance evaluation of PPP has been handled in various areas ranging from precision, accuracy, convergence period, to satellite visibility (Andrei, Salazar, and Chen, 2010). However, the long convergence periods still demand some remedies. Multi GNSS constellations, increasing the accuracy of real-time satellite orbit and clock corrections, and making sure that real-time atmospheric corrections are available by global/regional argumentation systems have been utilised in alleviating long convergence times in PPP (Pan et al., 2017; Rong-Xin et al., 2013; Song and Hao, 2016). Juan et al. (2012) further break down the atmospheric corrections into ionosphere-free combinations algorithms and precise real-time ionosphere delays. Klobuchar model and Global Ionosphere Maps (GIM) have been utilised in mitigating the ionosphere delay on measurements in single-frequency PPP. The magnitude of mitigation by the Klobuchar model is only 50-60% of total ionosphere effects (Rizos et al., 2012). The PPP performance as a consequence of the implementation of GIM in a PPP model outweighs that of Klobuchar model (Øvstedal, 2002).

Single-frequency and dual-frequency PPP ranging from single to multi-GNSS constellations show better results when multiple constellations are incorporated in either case. Despite the satisfying performance in multi-GNSS PPP, single-frequency PPP is still disadvantaged due to lack of full mitigation of ionosphere effects (Chen and Gao, 2005). In single-frequency PPP, the performance of GLONASS-only PPP is usually much worse than that of GPS-only. This is evidenced in Guo et al. (2017) and is as a result of pseudorange Inter-Frequency Biases (IFBs) and diminished accuracy of the published GLONASS ephemeris.

Lou et al. (2016) analyzed the contribution of Multi-GNSS PPP solution to single and dual-frequency raw observations based on 105 Multi-GNSS Experiment (MGEX) stations. This study was based on the analysis on convergence period and the positioning performance of PPP with raw single and dual-frequency data. The accuracy of multi-GNSS PPP has also been examined in for example Li et al. (2015a) and Li et al. (2015b). Chen et al. (2016) evaluated the accuracy of combined GPS+BDS PPP by comparing the kinematic and static PPP positions to the IGS daily solutions. In a similar study, Cai and Gao (2013) processed a static dataset from 511 IGS-MGEX stations and yielded a more improved convergence time but in GPS+GLONASS combination than in individual constellation. The integration GPS and

Ionospheric-Constrained PPP using Triple-GNSS Constellations (9769)
Robert Suya (Malawi)

FIG Working Week 2019
Geospatial information for a smarter life and environmental resilience
Hanoi, Vietnam, April 22–26, 2019

Galileo improves the PPP convergence time than in GPS-only PPP solution (Afifi and El-Rabbany, 2015; Rabbou and El-Rabbany, 2015). The input of Galileo to multi-GNSS has been demonstrated in Pan et al. (2017a) and Xia et al. (2018). Tegedor, Øvstedal and Vigen (2014) come up with improved PPP performance in the fusion of GPS and BDS than in GPS-only PPP.

Pan et al. (2017b) and Zhao et al. (2017) gathered more improved average convergence in 3D based on different combinations of GPS, GLONASS, Galileo, and BeiDou constellations than in GPS-only PPP. Abd Rabbou and El-Rabbany (2017) came up with an improvement in positional accuracies of 18% in GPS+BDS combination, 20% in GPS+Galileo and 13% in multi-constellation GNSS PPP with respect to GPS-only constellation. Yigit et al. (2014) unveiled the contribution of dual-frequency PPP in the integration GPS and GLONASS PPP solution. This study yielded better positioning performance and convergence time in the combined GNSS than in GPS-only PPP.

A recent investigation on multi-GNSS PPP using undifferenced and uncombined observations was limited to the Satellite POsitioning Service (SAPOS) stations located in Germany and involved only GPS+GLONASS GNSS constellations (Zhou et al., 2018). Further to that, Galileo GNSS has proved significant in accelerating convergence time, improving positioning accuracy, and in stabilising inter-system biases (ISBs) in multi-GNSS constellation (Xia et al., 2018). Considering the global contribution of Galileo to multi-GNSS, is it thus worthwhile to compensate the recent studies by evaluating the ionosphere-constrained PPP using Triple-GNSS constellations of GPS, GLONASS and Galileo. In this contribution, standard single-frequency PPP and dual-frequency PPP are analysed in kinematic mode in terms of convergence period.

2. GNSS OBSERVATION MODELS

2.1 Linearized Observation Equation

The GNSS pseudorange (Equation 1) and carrier phase (Equation 2) linearized observations models are expressed in Leick et al. (2015 as:

$$p_{r,j}^{s,T} = u_r^{s,T}.x + dt_r - dt^{s,T} + M_W.Z_W + \gamma_j^T.I_{r,1}^{s,T} + \left(d_{r,j}^{s,T} - d_j^{s,T}\right) + \varepsilon_{r,j}^{s,T} \qquad [1]$$

$$l_{r,j}^{s,T} = u_r^{s,T}.x + dt_r - dt^{s,T} + M_W.Z_W - \gamma_j^T.I_{r,1}^{s,T} + \lambda_j^{s,T}.\left(N_{r,j}^{s,T} + b_{r,j}^{s,T} - b_j^{s,T}\right) + \varepsilon_{r,j}^{s,T} \qquad [2]$$

$$\gamma_j^T = \left(f_1^{s,T} / f_j^{s,T}\right)^2 \qquad [3]$$

The notation in [1], [2] and [3] is as follows: p denotes pseudorange; l denotes carrier phase; the indices r, s and j represent receiver, satellite and carrier frequency band (1, 2), respectively; and the superscript T denotes any GNSS such that $T \in \{G, R, E, ...\}$, for GPS, GLONASS, Galileo, etc. ; $p_{r,1}^{1,T}$ and $l_{r,1}^{1,T}$ are vectors of **O**bserved **M**inus **C**omputed (OMC)

Ionospheric-Constrained PPP using Triple-GNSS Constellations (9769)
Robert Suya (Malawi)

FIG Working Week 2019
Geospatial information for a smarter life and environmental resilience
Hanoi, Vietnam, April 22–26, 2019

values of pseudorange and carrier-phase observables, respectively; $u_r^{s,T}$ is the satellite-receiver unit vector; x denotes the receiver position increments with respect to the a priori position; dt_r and $dt^{s,T}$ denote the receiver and satellite clock drifts, respectively; M_W is the wet mapping function; Z_W is the zenith wet delay; $I_{r,1}^{s,T}$ is the line-of-sight (LOS) ionosphere delay on the frequency ($f_1^{s,T}$); γ_j^T is the frequency-dependent multiplier factor as defined in Equation 3; $d_{r,j}^{s,T}$ and $d_j^{s,T}$ are the frequency-dependent receiver **U**ncalibrated **C**ode **D**elay (UCD) with respect to satellite s and frequency-dependent satellite UCD, respectively; $\lambda_j^{s,T}$ denotes the carrier wavelength on the frequency band j; $N_{r,j}^{s,T}$ denotes the integer phase ambiguity from satellite s to receiver r of satellite system T on frequency band j; $b_{r,j}^{s,T}$ and $b_j^{s,T}$ denote the frequency-dependent receiver and satellite **U**ncalibrated **P**hase **D**elays (UPDs); $\varepsilon_{r,j}^{s,T}$ represents the measurement noise and multipath error.

2.2 Generation of Precise Ephemeris

Kouba and Héroux (2001) express an equation for the generation of precise ephemeris using ionosphere-free (IF) observables by International GNSS Service as:

$$dt_{IF}^{s,T} = dt^{s,T} + \left(\alpha_{12}^T . d_1^{s,T} + \beta_{12}^{s,T} . d_2^{s,T} \right) \qquad [4]$$

Equation [1] and [2] simplify to [5] and [6] when the IGS precise orbit and clocks are applied:

$$\begin{cases} p_{r,1}^{s,T} = u_r^{s,T}.x + dt_r + d_{r,1}^{s,T} + M_W.Z_W + I_{r,1}^{s,T} - \beta_{12}^T.DCB_{P1P1}^{s,T} + \varepsilon_{r,1}^{s,T} \\ p_{r,2}^{s,T} = u_r^{s,T}.x + dt_r + d_{r,2}^{s,T} + M_W.Z_W + \gamma_2^T.I_{r,1}^{s,T} + \alpha_{12}^T.DCB_{P1P2}^{s,T} + \varepsilon_{r,2}^{s,T} \end{cases} \qquad [5]$$

$$\begin{cases} l_{r,1}^{s,T} = u_r^{s,T}.x + dt_r + M_W.Z_W - I_{r,1}^{s,T} + d_{IF_{12}}^{s,T} + \lambda_1^{s,T}.\left(N_{r,1}^{s,T} + b_{r,1}^{s,T} - b_1^{s,T} \right) + \zeta_{r,1}^{s,T} \\ l_{r,2}^{s,T} = u_r^{s,T}.x + dt_r + M_W.Z_W - I_{r,1}^{s,T} + d_{IF_{12}}^{s,T} + \lambda_2^{s,T}.\left(N_{r,2}^{s,T} + b_{r,2}^{s,T} - b_2^{s,T} \right) + \zeta_{r,2}^{s,T} \end{cases} \qquad [6]$$

2.3 Receiver and Satellite Biases

Receiver hardware biases vary for each satellite system and this difference between signals of different constellations is referred to as intersystem bias (ISB)(Teunissen and Montenbruck, 2017). For the four existing GNSS, three (GPS, Galileo, and BeiDou) employ Code Division Multiple Access (CDMA) and one (GLONASS) utilises Frequency Division Multiple Access (FDMA). It is worth mentioning that, the disparity in frequency between satellite hardware biases is termed as inter-frequency biases (IFBs) or differential code biases (DCBs). GNSS PPP algorithm has a bearing on whether to apply the DCBs or not. For instance, in a standard PPP algorithm, it is optional to correct satellite DCBs, whereas in ionosphere-constrained PPP

Ionospheric-Constrained PPP using Triple-GNSS Constellations (9769)
Robert Suya (Malawi)

FIG Working Week 2019
Geospatial information for a smarter life and environmental resilience
Hanoi, Vietnam, April 22–26, 2019

algorithm, satellite DCBs must be corrected in advance (Zhou et al., 2018). Table 1 depicts the sources of DCBs from MGEX.

Table 1: Multi-GNSS Orbits and Clocks FROM MGEX.

Provider	Identity	Constellation	GNSS Product
CODE	com	G + R + E + C + J	sp3, clk, erp, bia
	COD0MGXFIN	G + R + E + C + J	
GFZ	gfm / gbm	G + R + E + C + J	sp3, clk, erp, bia
TUM	tum	E + J	sp3, clk, erp
Wuhan University	wum	G + R + E + C + J	sp3, clk, erp
CNES	grm	G + R + E	sp3, clk, snx
JAXA	qzf	G + J	sp3
	JAX0MGXFIN	G + R + J	sp3

Key: The bia, erp, snx, and sp3 denote biases, earth rotation parameters, sinex (containing site coordinates), and standard product 3, respectively (http://mgex.igs.org/IGS_MGEX_Products.php).

2.4 Standard Single-Frequency and Ionosphere-Constrained Single-Frequency PPP

The standard single-frequency PPP does not take into account virtual observations for ionosphere parameters whereas the ionosphere-constrained single-frequency PPP does (Teunissen & Montenbruck, 2017). Virtual observations are simply pseudo-observations which are used to add constraint on some estimated parameter(s) such as ionospheric delay or tropospheric delay parameter (Yao, Yu, & Hu, 2014).

The standard single-frequency PPP model is expressed in [7] and [8] which is simply a matrix representation of [5] and [6]. Similarly, the ionosphere-constrained single-frequency PPP is presented in [9]:

$$
\begin{bmatrix} p_{r,1}^{1,T} \\ l_{r,1}^{1,T} \\ \vdots \\ p_{r,1}^{m,T} \\ l_{r,1}^{m,T} \end{bmatrix} = \begin{bmatrix} -u & 1 & M_W & K & R_1 \end{bmatrix} \begin{bmatrix} x \\ d\bar{t}_r^T \\ Z_W \\ I_{r,1}^T \\ \bar{N}_{r,1}^T \end{bmatrix} + \begin{bmatrix} \varepsilon_{r,1}^T \\ \xi_{r,1}^T \end{bmatrix}, Q_L \tag{7}
$$

$$
\begin{cases} d\bar{t}_r^T = dt_r + d_{r,1}^T \\ \bar{N}_{r,1}^{s,T} = \lambda_1^T.\left(N_{r,1}^{s,T} + b_{r,1}^{s,T} - b_1^{s,T}\right) + d_{IF_{12}}^{s,T} - d_{r,1}^T \end{cases} \tag{8}
$$

Ionospheric-Constrained PPP using Triple-GNSS Constellations (9769)
Robert Suya (Malawi)

FIG Working Week 2019
Geospatial information for a smarter life and environmental resilience
Hanoi, Vietnam, April 22–26, 2019

The definitions for the notations in [7] and [8] are as follows:

m the number of satellites; 1 is a vector of **2** x **m** rows and a single column with each element equal to one corresponding to the receiver clock parameter ($d\bar{t}_{r,T}$); the element for the corresponding $p_{r,1}^{s,T}$ is 1 whereas that of $l_{r,1}^{s,T}$ is -1 corresponding to the ionosphere parameter ($I_{r,1}^{T}$) in matrix K; R_1 is the matrix corresponding to the ambiguity parameter ($\bar{N}_{r,1}^{T}$); the element for the corresponding $p_{r,1}^{s,T}$ is 0, whereas $l_{r,1}^{s,T}$ is 1; O is the null matrix; Q_L is the stochastic model of the OMC observables, and Q_I is the stochastic model for the virtual ionospheric observables.

$$
\begin{bmatrix} p_{r,1}^{1,T} \\ l_{r,1}^{1,T} \\ \vdots \\ p_{r,1}^{m,T} \\ l_{r,1}^{m,T} \\ \tilde{I}_{r,1}^{1,T} \\ \vdots \\ \tilde{I}_{r,1}^{m,T} \end{bmatrix} = \begin{bmatrix} -u & 1 & M_W & K & R_1 \\ O & O & O & I & O \end{bmatrix} \begin{bmatrix} x \\ d\bar{t}_r^{T} \\ Z_W \\ I_{r,1}^{T} \\ \bar{N}_{r,1}^{T} \end{bmatrix} + \begin{bmatrix} \varepsilon_{r,1}^{T} \\ \xi_{r,1}^{T} \\ \varepsilon_{r,ion}^{T} \end{bmatrix}, Q_L, Q_I \qquad [9]
$$

In [9], for satellite **s**, $\tilde{I}_{r,1}^{s,T}$ may be derived from a couple of sources: GIM (Hernández-Pajares et al., 2009) and regional ionosphere models (RIM) (Yao et al., 2013). In a PPP algorithm, users can apply GIM or RIM as a constraint of correcting ionospheric delay.

2.5 Standard Dual-Frequency and Ionosphere-Constrained Dual-Frequency PPP

The standard dual-frequency PPP absorbs uncalibrated code delays (UCDs) for both the receiver clock offset and line of sight ionosphere delay parameters. This distinguishes it from the standard single-frequency PPP where only receiver UCDs can be absorbed by the receiver clock offset. The standard dual-frequency PPP are presented in [10] and [11] and ionosphere-constrained dual-frequency in [10] and [11].

$$
\begin{bmatrix} p_{r,1}^{1,T} \\ l_{r,1}^{1,T} \\ \vdots \\ p_{r2}^{m,T} \\ l_{r,2}^{m,T} \end{bmatrix} = \begin{bmatrix} -u & 1 & M_W & K & R_1 & R_2 \end{bmatrix} \begin{bmatrix} x \\ d\bar{t}_r^{T} \\ Z_W \\ I_{r,1}^{T} \\ \bar{N}_{r,1}^{T} \\ \bar{N}_{r,2}^{T} \end{bmatrix} + \begin{bmatrix} \varepsilon_{r,1}^{T} \\ \xi_{r,1}^{T} \end{bmatrix}, Q_L \qquad [10]
$$

Ionospheric-Constrained PPP using Triple-GNSS Constellations (9769)
Robert Suya (Malawi)

FIG Working Week 2019
Geospatial information for a smarter life and environmental resilience
Hanoi, Vietnam, April 22–26, 2019

$$\begin{cases} d\bar{t}_r^{\,T} = dt_r + d_{r,IF_{12}}^T \\ I_{r,1}^{s,T} = I_{r,1}^{s,T} + \beta_{12}^T.\left(DCB_{r,P1P2}^T - DCB_{r,P1P2}^{s,T}\right) \\ \bar{N}_{r,1}^{s,T} = \lambda_1^T.\left(N_{r,1}^{s,T} + b_{r,1}^{s,T} - b_1^{s,T}\right) + d_{IF_{12}}^{s,T} - d_{r,IF_{12}}^{s,T} + \beta_{12}^T.\left(DCB_{r,P1P2}^T - DCB_{r,P1P2}^{s,T}\right) \\ \bar{N}_{r,1}^{s,T} = \lambda_2^T.\left(N_{r,2}^{s,T} + b_{r,2}^{s,T} - b_2^{s,T}\right) + d_{IF_{12}}^{s,T} - d_{r,IF_{12}}^{s,T} + \gamma_2^T.\beta_{12}^T.\left(DCB_{r,P1P2}^T - DCB_{r,P1P2}^{s,T}\right) \end{cases} \quad [11]$$

The implementation of the ionosphere-constrained dual-frequency is similar to that of the ionosphere-constrained single-frequency PPP. Both add virtual observations for ionosphere parameters and their corresponding constraints to the observation models. However, the application of DCBs in dual-frequency model distinguishes it from the single-frequency PPP model. Notwithstanding that, the [10] and [12] have a R_2 matrix that corresponds to the ambiguity parameters ($\bar{N}_{r,2}^T$) while $p_{r,2}^{s,T}$ and $l_{r,2}^{s,T}$ corresponds to 0 and 1, respectively.

$$\begin{bmatrix} p_{r,1}^{1,T} \\ l_{r,1}^{1,T} \\ \vdots \\ p_{r,2}^{m,T} \\ l_{r,2}^{m,T} \\ \tilde{I}_{r,1}^{1,T} \\ \vdots \\ \tilde{I}_{r,1}^{m,T} \end{bmatrix} = \begin{bmatrix} -u & 1 & J & M_W & K & R_1 & R_2 \\ O & O & O & O & I & O & O \end{bmatrix} \begin{bmatrix} x \\ d\bar{t}_r^{\,T} \\ DCB_{r,P1P2}^T \\ Z_W \\ I_{r,1}^T \\ \bar{N}_{r,1}^T \\ \bar{N}_{r,2}^T \end{bmatrix} + \begin{bmatrix} \varepsilon_{r,1}^T \\ \xi_{r,1}^T \\ \varepsilon_{r,ion}^T \end{bmatrix}, Q_L, Q_I \quad [12]$$

$$\begin{cases} \bar{N}_{r,1}^{s,T} = \lambda_1^T.\left(N_{r,1}^{s,T} + b_{r,1}^{s,T} - b_1^{s,T}\right) + d_{IF_{12}}^{s,T} - d_{r,IF_{12}}^{s,T} \\ \bar{N}_{r,1}^{s,T} = \lambda_2^T.\left(N_{r,2}^{s,T} + b_{r,2}^{s,T} - b_2^{s,T}\right) + d_{IF_{12}}^{s,T} - d_{r,IF_{12}}^{s,T} \end{cases} \quad [13]$$

For J matrix, $p_{r,1}^{s,T}$ corresponds to β_{12}^T whereas the element for $p_{r,2}^{s,T}$ is $-\alpha_{12}^T$ that corresponds to $DCB_{r,P1P2}^T$.

2.6 Triple-GNSS Constellation PPP Processing

2.6.1 Datasets

To perform a thorough evaluation of ionosphere-constrained PPP using triple-GNSS constellations, GPS+GLONASS+Galileo GNSS constellations are evaluated in kinematic mode over nine (9) Multi-GNSS Experiment (MGEX) stations located in Africa (and part of

Ionospheric-Constrained PPP using Triple-GNSS Constellations (9769)
Robert Suya (Malawi)

FIG Working Week 2019
Geospatial information for a smarter life and environmental resilience
Hanoi, Vietnam, April 22–26, 2019

Spain). The selected stations are illustraated in Figure 1. Twenty-four (24) hour observations from DOY 032 to DOY 038 (first week of February, 2017) are processed in four PPP scenarios: GPS-only, GLONASS-only, GPS+GLONASS, and triple-constellation of GPS+GLONASS+Galileo at 7° elevation angle cut-off (Table 2).

Table 2: Summary of MGEX stations selected for the study

SN	Site	Country	Latititude (DD)	Longitude (DD)	Height (m)	Constellation
1	DJIG00DJI	Djibouti	11.526	42.847	711.409	GPS+GLO+GAL+BDS+SBAS
2	HARB00ZAF	South Africa	-25.887	27.707	1558.078	GPS+GLO+GAL+BDS+SBAS+IRNSS
3	MAL200KEN	Kenya	-2.996	40.194	-20.400	GPS+GLO+GAL+BDS+SBAS
4	MELI00ESP	Spain	35.281	-2.952	93.000	GPS+GLO+GAL
5	MOIU00KEN	Kenya	0.288	35.290	2201.532	GPS+GLO+GAL+BDS+IRNSS
6	NKLG00GAB	Gabon	0.354	9.672	31.496	GPS+GLO+GAL+BDS+SBAS
7	SUTM00ZAF	South Africa	-32.381	20.811	1797.600	GPS+GLO+GAL
8	VOIM00MDG	Madagascar	-21.906	46.793	1163.300	GPS+GLO+GAL
9	ZAMB00ZMB	Zambia	-15.426	28.311	1324.914	GPS+GLO+GAL

Key: DD stands for Decimal Degrees

The quality of orbits and clocks applied in a PPP model influences the PPP positioning performance (for example, Lou et al., 2014; Lou et al., 2015). Table 1 above depicts the multi-GNSS constellation precise satellite orbit and clock products commonly applied in PPP. Astudillo et al. (2018) used WUM precise satellite orbit and clock products in POINT (Position And Navigation Data Analyst) command-line software. The precise ephemeris generated in analysis centres (ACs) are proven to be in agreement with those provided by the Deutsches GeoForschungsZentrum (GFZ)(Guo et al., 2017a; 2017b). With this negligible difference in orbit and clock products generated by different ACs, this paper applies the GFZ precise ephemeris.

2.6.1 Data Processing Strategy

In order to investigate the Ionosphere-constrained PPP using triple-GNSS constellations of GPS, GLONASS and Galileo, a GNSS Analysis software for Multi-constellation and multi-frequency Precise positioning (GAMP) was utilised. GAMP is a command line software capable of performing multi-GNSS PPP based on undifferenced and uncombined observations developed by Zhou et al.(2018).

Ionospheric-Constrained PPP using Triple-GNSS Constellations (9769)
Robert Suya (Malawi)

FIG Working Week 2019
Geospatial information for a smarter life and environmental resilience
Hanoi, Vietnam, April 22–26, 2019

Table 3: Data processing strategy

Parameter	Description
Position Mode	Kinematic PPP
Filter Processing Mode	Backward
Constellation	[G], [R], [G + R], and [G + R + E]
Elevation Cut-Off Angle	7°
Sampling Rate	30 seconds
Frequencies	Single/Dual
Ionospheric Constraint	On/Off
Ionospheric Delay Estimation	Random Walk
MGEX Orbits and Clocks	Deutsches GeoForschungsZentrum (GFZ)
Receiver/Satellite Antenna PCO and PCV	IGS ANTEX (IGS14.atx)
Phase Wind-Up Effect	IERS conventions 2010
Tropospheric Mappng Function	Global Mapping Function (GMF)
Tide Correction	Solid earth Tide, Ocean Loading Tide and Pole Tide

Key: G, R, E and C stand for GPS, GLONASS, Galileo and BeiDou navigation systems. PCO and PCV stand for Phase Center Offset and Phase Center Variation, respectively. ANTEX denotes Antenna Exchange Format.
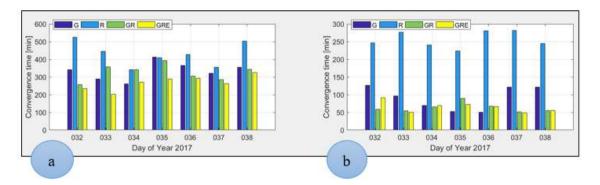
The parameters provided in the IGS ANTEX (IGS14.atx) were used in collecting the satellite and reciver Phase Center Offsets (PCO) and Phase Center Variations (PCV). Multi-GNSS constellation precise satellite orbit and clock products from MGEX were applied to mitigate the satellite orbit and clock errors. Backward smoothing was used in order to assess the solution after ambiguity convergence for the kinematic PPP solutions (Teunissen & Montenbruck, 2017). Table 2 depicts the data processing strategy and model for triple-GNSS PPP implemented in this study. The average convergence time and standard deviation for the single and dual-frequency PPP solutions are computed.

3. RESULTS AND ANALYSIS

3.1 Single-Frequency PPP and Ionosphere-Constrained Single-Frequency PPP

The average convergence time for the standard single-frequency PPP (a) and ionosphere-constrained PPP (b) is illustrated in Figure 2. As can be seen in Figure 2a, the average convergence time for the integration of GPS+GLONASS PPP solutions in (a) is considerably better than that of GPS-only PPP by about 9 min (Table 3). Similarly, the triple-constellation GNSS (GRE) has an average convergence time of about 269 minutes and an overall standard deviation of 41 min. This indicates an improvement of about 20% in convergence time with respect to GPS-only PPP solution (Table 3).

Ionospheric-Constrained PPP using Triple-GNSS Constellations (9769)
Robert Suya (Malawi)

FIG Working Week 2019
Geospatial information for a smarter life and environmental resilience
Hanoi, Vietnam, April 22–26, 2019

Figure 1: Average convergence time for standard single-frequency PPP (a) and ionosphere-constrained single-frequency PPP (b) per day.

The average convergence performance of GLONASS-only PPP is poorer (429 min) than that of GPS-only PPP (335 min). The pseudorange IFBs and reduced accuracy of GLONASS orbits and clocks may provide justification to the poor convergence time in GLONASS-only PPP solution (Guo et al., 2017a).

The performance of GLONASS-only PPP in the ionosphere-constrained approach is substantially improved by about 40% (from 429.2 min to 256.4 min) in relation to standard single-frequency PPP. Here, the Global Ionosphere Maps (GIM) generated on a daily basis at CODE (Center for Orbit Determination in Europe) using MGEX datasets are applied in a PPP algorithm. The other three PPP scenarios: GPS-only, GPS+GLONASS, and GPS+GLONASS+Galileo improve by 73%, 81% and 76%, respectively. It is apparent that the convergence time in GLONASS-only PPP is improved by less than 50%. This may be attributed to strong correlation between LOS ionosphere delays and pseudorange IFBs (Zhou et al., 2018a; Zhou et al., 2018b).

The addition of GLONASS to GPS-only PPP solution improves the convergence time by 30% from 91.2 min to 63.4 min (Figure 2b). The convergence time improves further as a consequence of the triple-constellation of GPS+GLONASS+Galileo by about 29%, comparing to GPS-only PPP solution (Table 3). This is attributed to increased number of satellites in the GPS+GLONASS+Galileo kinematic PPP than in GPS-only PPP.

3.2 Dual-Frequency PPP and Ionosphere-Constrained Dual-Frequency PPP

The average convergence time for the standard dual-frequency PPP (a) and ionosphere-constrained PPP (b) is illustrated in Figure 3. The corresponding statistical summary is presented in Table 3. The standard dual-frequency PPP performed better in all the PPP scenarios as indicated by small magnitude of average convergence times in Table 3. As can be evidenced in Figure 3 and Table 3, the convergence time is improved by 53% in triple-GNSS constellation, comparing to GPS-only PPP (from 42 min to 20 min). The standard deviation as a result of triple-constellation also rises from about 18 min to 3 min.
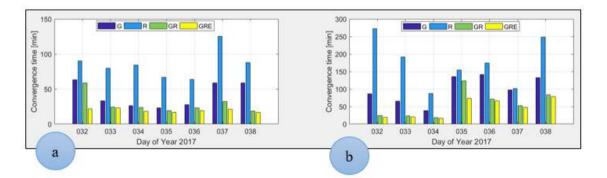
Ionospheric-Constrained PPP using Triple-GNSS Constellations (9769)
Robert Suya (Malawi)

FIG Working Week 2019
Geospatial information for a smarter life and environmental resilience
Hanoi, Vietnam, April 22–26, 2019

The implementation of the GIM in the ionosphere-constrained PPP results in reduced performance as compared to the standard dual-frequency PPP. This is apparently indicated by longer convergence times (Table 3) in the ionosphere-constrained PPP. The thresholds for the convergence time for G, R, GR, and GRE and their associated standard deviations have been expressed in minutes.

Table 4: Statistics for single and dual-frequency PPP solutions.

Parameter (min)	G	R	GR	GRE	Description
Mean	334.9	429.2	326.0	268.6 [19.8%]	SF
SD	50.3	69.2	45.9	40.6	SF
Mean	91.2	256.4	63.4	65.1 [28.6%]	SF-IC
SD	33.5	23.1	12.8	15.2	SF-IC
Mean	41.5	85.4	28.6	19.7 [52.5%]	DF
SD	17.8	20.2	14.0	2.6	DF
Mean	99.6	175.8	56.7	46.2 [53.7%]	DF-IC
SD	39.4	69.2	38.8	27.0	DF-IC

Key: SD denotes standard deviation; SF denotes single frequency; IC denotes ionosphere-constrained; DF denotes dual frequency. G,R,GR, and GRE denote GPS, GLONASS, GPS+GLONASS, GPS+GLONASS+Galileo, respectively. The percentages in the square brankets indicate the rate of improvement (in convergence time) in the triple-GNSS constellation PPP with respect to GPS-only PPP solution.

Figure 2: Average convergence time for standard dual-frequency PPP (a) and ionosphere-constrained dual-frequency PPP (b) per day.

It can be discerned that the GIM in the dual-frequency ionosphere-constrained PPP impairs the overall convergence time. This is contrary to the single-frequency PPP with virtual observations. Despite the longer convergence time in Figure 3b, the individual constellation experience satisfying degree of improvement. For instance, with corresponding standard deviations of 39 min and 27 min, the average convergence gets better by 43% and 54% in GPS+GLONASS and triple-GNSS constellation, respectively. The convergence time of the

Ionospheric-Constrained PPP using Triple-GNSS Constellations (9769)
Robert Suya (Malawi)

FIG Working Week 2019
Geospatial information for a smarter life and environmental resilience
Hanoi, Vietnam, April 22–26, 2019

triple-GNSS constellation outweighs that of dual and single-GNSS system. The improvement may be due to the addition of Galileo satellites to the dual-constellation of GPS+GLONASS.

4. CONCLUSIONS

In this paper, the ionosphere-constrained PPP using triple-GNSS constellations was evaluated in terms of convergence period. The triple-GNSS constellations of GPS+GLONASS+Galileo ware assessed in four different PPP scenarios: GPS-only, GLONASS-only, GPS+GLONASS and GPS+GLONASS+Galileo in kinematic mode over nine (9) Multi-GNSS Experiment (MGEX) stations located in Africa (and part of Spain). To validate the results, the ionosphere-constrained PPP was analysed in both single and dual-frequency. Based on the results, the following conclusions are drawn:

1) The application of GIM in ionosphere-constrained PPP improves the overall convergence time and standard deviation with respect to standard single-frequency PPP.
2) The convergence performance of dual-frequency is considerably much better without virtual observations.
3) There is improved average convergence time in triple-GNSS constellation PPP in comparison with GPS-only PPP in standard single and dual-frequency PPP, and in ionosphere-constrained PPP.

This study unveils the threshold of performance for the ionosphere-constrained PPP using triple-GNSS constellations. However, the study was limited to triple-GNSS and MGEX stations located in Africa (and part of Spain). A similar study may be performed by comparing the performance using DCBs from different providers.

REFERENCES

Abd-Rabbou, M., and El-Rabbany, A. (2017). Performance analysis of precise point positioning using multi-constellation GNSS : GPS , GLONASS , Galileo and BeiDou, *6265*(May 2016). https://doi.org/10.1080/00396265.2015.1108068

Afifi, A., and El-Rabbany, A. (2015). Performance analysis of several GPS/Galileo precise point positioning models. *Sensors (Switzerland)*, *15*(6), 14701–14726. https://doi.org/10.3390/s150614701

Andrei, C.O., Salazar, D., and Chen, R. (2010). Performance Analysis of the Precise Point Positioning Technique at BUCU IGS Station. *RevCAD – Journal of Geodesy and Cadastre*, *10*, 9–20. Retrieved from http://www.uab.ro/geocad/upload/19_107_Paper1_RevCAD10_2010.pdf

Astudillo, J. M., Lau, L., Tang, Y. T., and Moore, T. (2018). Analysing the Zenith

Ionospheric-Constrained PPP using Triple-GNSS Constellations (9769)
Robert Suya (Malawi)

FIG Working Week 2019
Geospatial information for a smarter life and environmental resilience
Hanoi, Vietnam, April 22–26, 2019

tropospheric delay estimates in on-line precise point positioning (PPP) services and PPP software packages. *Sensors (Switzerland)*, *18*(2). https://doi.org/10.3390/s18020580

Cai, C., and Gao, Y. (2013). Modeling and assessment of combined GPS/GLONASS precise point positioning. *GPS Solutions*, *17*(2), 223–236. https://doi.org/10.1007/s10291-012-0273-9

Chen, J., Wang, J., Zhang, Y., Yang, S., Chen, Q., and Gong, X. (2016). Modeling and assessment of GPS/BDS combined precise point positioning. *Sensors (Switzerland)*, *16*(7). https://doi.org/10.3390/s16071151

Chen, K., and Gao, Y. (2005). Real-Time Precise Point Positioning Using Single Frequency Data. *Proceedings of the 18th International Technical Meeting of the Satellite Division of The Institute of Navigation (ION GNSS 2005)*.

Guo, F., Li, X., Zhang, X., and Wang, J. (2017a). Assessment of precise orbit and clock products for Galileo, BeiDou, and QZSS from IGS Multi-GNSS Experiment (MGEX). *GPS Solutions*, *21*(1), 279–290. https://doi.org/10.1007/s10291-016-0523-3

Guo, F., Li, X., Zhang, X., and Wang, J. (2017b). The contribution of Multi-GNSS Experiment (MGEX) to precise point positioning. *Advances in Space Research*, *59*(11), 2714–2725. https://doi.org/10.1016/j.asr.2016.05.018

Guo, F., Li, X., Zhang, X., and Wang, J. (2017c). The contribution of Multi-GNSS Experiment (MGEX) to precise point positioning. *Advances in Space Research*. https://doi.org/10.1016/j.asr.2016.05.018

Hernández-Pajares, M., Juan, J. M., Sanz, J., Orus, R., Garcia-Rigo, A., Feltens, J., … Krankowski, A. (2009). The IGS VTEC maps: A reliable source of ionosphere information since 1998. *Journal of Geodesy*. https://doi.org/10.1007/s00190-008-0266-1

Huber, K., Heuberger, F., Abart, C., Karabatic, A., and Berglez, P. (2010). PPP : Precise Point Positioning – Constraints and Opportunities. *FIG Congress - Facing Challenges - Building the Capacity*, (GNSS Modernisation and Trends), 11–16.

Juan, J. M., Hernández-Pajares, M., Sanz, J., Ramos-Bosch, P., Aragón-Ángel, A., Orús, R., … Tossaint, M. (2012). Enhanced Precise Point Positioning for GNSS users. *IEEE Transactions on Geoscience and Remote Sensing*, *50*(10 PART2), 4213–4222. https://doi.org/10.1109/TGRS.2012.2189888

Kouba, J., and Héroux, P. (2001). Precise Point Positioning Using IGS Orbit and Clock Products. *GPS Solutions*. https://doi.org/10.1007/PL00012883

Li, X., Ge, M., Dai, X., Ren, X., Fritsche, M., Wickert, J., and Schuh, H. (2015). Accuracy and reliability of multi-GNSS real-time precise positioning: GPS, GLONASS, BeiDou, and Galileo. *Journal of Geodesy*, *89*(6), 607–635. https://doi.org/10.1007/s00190-015-0802-8

Ionospheric-Constrained PPP using Triple-GNSS Constellations (9769)
Robert Suya (Malawi)

FIG Working Week 2019
Geospatial information for a smarter life and environmental resilience
Hanoi, Vietnam, April 22–26, 2019

Li, X., Zhang, X., Ren, X., Fritsche, M., Wickert, J., and Schuh, H. (2015). Precise positioning with current multi-constellation Global Navigation Satellite Systems: GPS, GLONASS, Galileo and BeiDou. *Scientific Reports*, *5*(1), 8328. https://doi.org/10.1038/srep08328

Li, X., Zus, F., Lu, C., Dick, G., Ning, T., Ge, M., … Schuh, H. (2015). Retrieving of atmospheric parameters from multi-GNSS in real time: Validation with water vapor radiometer and numerical weather model. *Journal of Geophysical Research*, *120*(14), 7189–7204. https://doi.org/10.1002/2015JD023454

Lou, Y., Zhang, W., Wang, C., Yao, X., Shi, C., Liu, J., (2014). The impact of orbital errors on the estimation of satellite clock errors and PPP. Adv. Space Res. 54 (8), 1571–1580.

Lou, Y., Zheng, F., Gu, S., Liu, Y., (2015). The impact of non-nominal yaw attitudes of GPS satellites on kinematic PPP solutions and their mitigation strategies. J. Navig. 68 (4), 718–734.

Lou, Y., Zheng, F., Gu, S., Wang, C., Guo, H., and Feng, Y. (2016). Multi-GNSS precise point positioning with raw single-frequency and dual-frequency measurement models. *GPS Solutions*, *20*(4), 849–862. https://doi.org/10.1007/s10291-015-0495-8

Øvstedal, O. (2002). Absolute Positioning with Single-Frequency GPS Receivers. *GPS Solutions*. https://doi.org/10.1007/PL00012910

Pan, L., Cai, C., Santerre, R., and Zhang, X. (2017b). Performance evaluation of single-frequency point positioning with GPS, GLONASS, BeiDou and Galileo. *Survey Review*, *49*(354), 197–205. https://doi.org/10.1080/00396265.2016.1151628

Pan, L., Zhang, X., Li, X., Li, X., Lu, C., and Liu, J., (2017a). Satellite availability and point positioning accuracy evaluation on a global scale for integration of GPS, GLONASS, BDS and Galileo. Adv. Space Res., 10.1016/j.asr.2017.07.029.

Rabbou, M. A., and El-Rabbany, A. (2015). Precise Point Positioning using Multi-Constellation GNSS Observations for Kinematic Applications. *Journal of Applied Geodesy*, *9*(1), 15–25. https://doi.org/10.1515/jag-2014-0021

Ren, X., Zhang, X., Xie, W., Zhang, K., Yuan, Y., and Li, X. (2016). Global Ionosphere Modelling using Multi-GNSS: BeiDou, Galileo, GLONASS and GPS. *Scientific Reports*, *6*. https://doi.org/10.1038/srep33499

Rizos, C., Janssen, V., Roberts, C., and Grinter, T. (2012). Precise Point Positioning: Is the Era of Differential GNSS Positioning Drawing to an End? *FIG Working Week 2012*, (May), 1–17. https://doi.org/http://www.gmat.unsw.edu.au/snap/publications/rizos_etal2012a.pdf

Rong-Xin, F., Chuang, S., Wei-Wei, S., Xiao-Ji, N., Quan, Z., Ke-Jie, C., and Jing-Nan, L. (2013). Real-time GNSS seismometer and its accuracy. *CHINESE JOURNAL OF*

Ionospheric-Constrained PPP using Triple-GNSS Constellations (9769)
Robert Suya (Malawi)

FIG Working Week 2019
Geospatial information for a smarter life and environmental resilience
Hanoi, Vietnam, April 22–26, 2019

GEOPHYSICS-CHINESE EDITION, *56*(2), 450–458. https://doi.org/10.6038/cjg20130209

Song, C., and Hao, J. ming. (2016). Accelerating the Convergence Speed of Precise Point Positioning by Using Multi-mode GNSS. *Chinese Astronomy and Astrophysics*, *40*(2), 247–255. https://doi.org/10.1016/j.chinastron.2016.05.006

Tegedor, J., Øvstedal, O., and Vigen, E. (2014). Precise orbit determination and point positioning using GPS, Glonass, Galileo and BeiDou. *Journal of Geodetic Science*, *4*(1). https://doi.org/10.2478/jogs-2014-0008

Teunissen, P. J. G., and Montenbruck, O. (2017). *Springer Handbook of Global Navigation Satellite Systems. Computers and electronics in agriculture*. https://doi.org/10.1007/978-3-319-42928-1

Vollath, U., Buecherl, A., Landau, H., Pagels, C., and Wagner, B. (2000). Multi-Base RTK Positioning Using Virtual Reference Stations. *Proceedings of the 13th International Technical Meeting of the Satellite Division of The Institute of Navigation (ION GPS 1998)*, 123–131. Retrieved from http://www.ion.org/search/view_abstract.cfm?jp=pandidno=1515

Xia, F., Ye, S., Xia, P., Zhao, L., Jiang, N., & Chen, D. (2018). Science Direct Assessing the latest performance of Galileo-only PPP and the contribution of Galileo to Multi-GNSS PPP. *Advances in Space Research*. https://doi.org/10.1016/j.asr.2018.06.008

Yao, Y., Zhang, R., Song, W., Shi, C., and Lou, Y. (2013). An improved approach to model regional ionosphere and accelerate convergence for precise point positioning. *Advances in Space Research*. https://doi.org/10.1016/j.asr.2013.07.020

Zhao, X., Wang, S., Liu, C., Ou, J., and Yu, X. (2017). Assessing the performance of multi-GNSS precise point positioning in Asia-Pacific region. *Survey Review*, *49*(354), 186–196. https://doi.org/10.1080/00396265.2016.1151576

Zhou, F., Dong, D., Ge, M., Li, P., Wickert, J., and Schuh, H. (2018b). Simultaneous estimation of GLONASS pseudorange inter-frequency biases in precise point positioning using undifferenced and uncombined observations. *GPS Solutions*, *22*(1). https://doi.org/10.1007/s10291-017-0685-7

Zhou, F., Dong, D., Li, W., Jiang, X., Wickert, J., and Schuh, H. (2018a). GAMP: An open-source software of multi-GNSS precise point positioning using undifferenced and uncombined observations. *GPS Solutions*, *22*(2). https://doi.org/10.1007/s10291-018-0699-9

Zumberge, J. F., Heflin, M. B., Jefferson, D. C., Watkins, M. M., and Webb, F. H. (1997). Precise point positioning for the efficient and robust analysis of GPS data from large networks. *Journal of Geophysical Research: Solid Earth*, *102*(B3), 5005–5017.

Ionospheric-Constrained PPP using Triple-GNSS Constellations (9769)
Robert Suya (Malawi)

FIG Working Week 2019
Geospatial information for a smarter life and environmental resilience
Hanoi, Vietnam, April 22–26, 2019

BIOGRAPHICAL NOTES

Robert Galatiya S.B. Suya is a lecturer in Geodesy and Geomatics Measurements Techniques (GMT) at the University of Malawi-The Polytechnic. His current research focuses on GMT, multi-GNSS PPP error modeling for high-precision positioning.

CONTACTS

Robert S.B. Galatiya Suya
University of Malawi-The Polytechnic
P/Bag 303
Chichiri
Blantyre 3
MALAWI
Email: rsuya@poly.ac.mw
Web site: https://www.poly.ac.mw/

Ionospheric-Constrained PPP using Triple-GNSS Constellations (9769)
Robert Suya (Malawi)

FIG Working Week 2019
Geospatial information for a smarter life and environmental resilience
Hanoi, Vietnam, April 22–26, 2019